Eur. Phys. J. A **10**, 365–371 (2001)

THE EUROPEAN PHYSICAL JOURNAL A

Coherent and incoherent π^0 photoproduction from the deuteron

U. Siodlaczek[1], P. Achenbach[2], J. Ahrens[3], J.R.M. Annand[8], H.-J. Arends[3], R. Beck[3], R. Bilger[1], H. Clement[1,a], V. Hejny[4], M. Kotulla[2], B. Krusche[7], V. Kuhr[5], R. Leukel[3], J.C. McGeorge[8], V. Metag[2], R. Novotny[2], V. Olmos de León[3], F. Rambo[5], M. Schepkin[6], A. Schmidt[3], I. Seluzhenkov[6,9], H. Ströher[4], G.J. Wagner[1], Th. Walcher[3], J. Weiß[2], F. Wissmann[5], and M. Wolf[2]

[1] Physikalisches Institut, Universität Tübingen, Auf der Morgenstelle 14, D-72076 Tübingen, Germany
[2] II. Physikalisches Institut, Universität Gießen, D-35392 Gießen, Germany
[3] Institut für Kernphysik, Universität Mainz, D-55099 Mainz, Germany
[4] Institut für Kernphysik, Forschungszentrum Jülich, D-52425 Jülich, Germany
[5] II. Physikalisches Institut, Universität Göttingen, D-37073 Göttingen, Germany
[6] Institute for Theoretical and Experimental Physics, Moscow 117218, Russia
[7] Institut für Physik und Astronomie, Universität Basel, Klingelbergstr. 82, CH-4056 Basel, Switzerland
[8] Department of Physics and Astronomy, University of Glasgow, Glasgow G128 QQ, UK
[9] Moscow State Engineering Physics Institute, Moscow 115409, Russia

Received: 13 February 2001 / Revised version: 11 April 2001
Communicated by M. Garçon

Abstract. Differential cross-sections for the reactions $d(\gamma,\pi^0)d$ and $d(\gamma,\pi^0)pn$ have been measured at MAMI with the TAPS detector setup in the energy range 140 MeV $< E_\gamma <$ 306 MeV. By use of the Glasgow tagging spectrometer an 0.8 MeV energy resolution for photons incident on the target was achieved. The π^0 missing energy resolution was sufficient for a reliable separation of coherent and incoherent channels. The data for the break-up channel exhibit very strong final state interaction effects, whereas the observed angular dependence of the inclusive process $d(\gamma,\pi^0)X$ is in quantitative agreement with predictions for a quasi-free process. The observed absolute $d(\gamma,\pi^0)X$ cross-sections, on the other hand, are significantly smaller than predicted by the quasi-free process for $E_\gamma \gtrsim 250$ MeV. Associating this failure with the π^0 photoproduction on the neutron would suggest that its cross-section is up to 25% below the presently believed value.

PACS. 13.60.Le Meson production – 25.20.Lj Photoproduction reactions

1 Introduction

Near threshold charged pion photoproduction from the nucleon is governed by the s-wave E_{0^+} amplitude originating from non-resonant Born terms. This process is strongly suppressed in π^0 production which is already dominated by the excitation of the Δ-resonance at threshold.

The pion photoproduction cross-sections are very well established for the proton; however, there are no corresponding data from direct measurements on the neutron for obvious reasons. The only source of information stems from measurements on nuclei, in particular on the deuteron, for which nuclear structure and medium effects are thought to be best under control.

Unlike the charged-pion case there are two reaction channels for π^0 production on the deuteron, the coherent channel $d(\gamma,\pi^0)d$, where the deuteron stays in its ground state (fig. 1a), and the so-called incoherent or break-up channel $d(\gamma,\pi^0)pn$, where the deuteron breaks up. The latter is thought to be dominated by the quasi-free process on the constituent nucleons (fig. 1b). However, as we will show below, the nucleon-nucleon final state interaction (NN-FSI) following the quasi-free process (fig. 1c) strongly influences the energy and angular dependence of the break-up channel. As we will also show, the modifications there turn out to be just counterbalanced by the

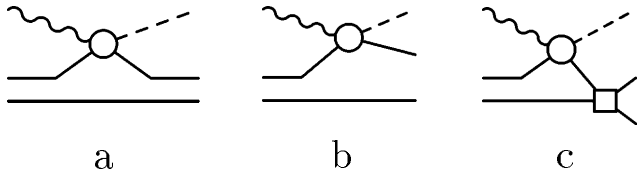

Fig. 1. Graphs representing the mechanisms for the π^0 production on the deuteron: (a) coherent process, (b) pure quasi-free process, (c) quasi-free process followed by NN-FSI.

[a] e-mail: clement@pit.physik.uni-tuebingen.de

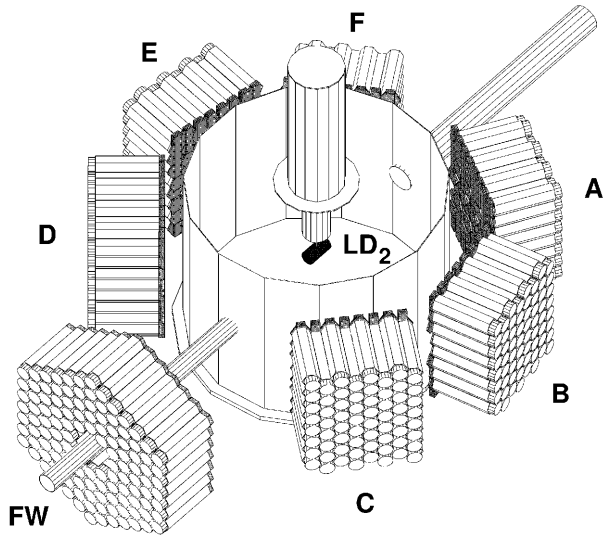

Fig. 2. TAPS detector setup at MAMI. Six TAPS blocks containing 8×8 BaF_2 modules each (A-F) and the forward wall containing 120 BaF_2-plastic phoswich modules (FW) are placed in plane around the target chamber containing the liquid deuterium target.

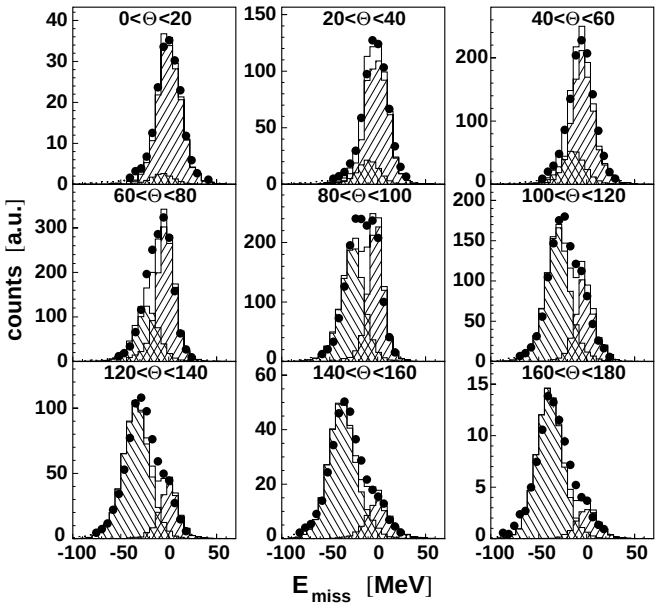

Fig. 3. Missing energy ($E_{\rm miss}$) spectra for the nine angular bins at $E_\gamma = 280$ MeV showing the distributions of coherent (forward sloped hatching) and incoherent (backward sloped hatching) events. The shapes of these distributions were obtained from MC simulations which reproduce the experimental resolution. Coherent and incoherent strengths were obtained from a fit (solid lines) to the experimental data (solid dots).

coherent channel, such that the quasi-free cross-section is recovered in the sum of both, which is the inclusive π^0 production cross-section. On this basis we will suggest an interesting modification of the $n(\gamma, \pi^0)$ cross-section.

2 Experiment

The measurements were carried out at MAMI using tagged photons in the energy range $E_\gamma = 140$–306 MeV with an energy resolution of $\Delta E_\gamma \approx 0.8$ MeV. The π^0 mesons emitted from the LD_2 target were detected via their 2γ decay using the TAPS detector as shown schematically in fig. 2. It comprises 6 blocks, each containing 64 hexagonal BaF_2 modules with individual plastic veto detectors, together with a forward wall containing 120 BaF_2-plastic phoswich telescopes. Compared to a previous investigation [1] of the same reaction which utilized 5 TAPS blocks but no forward wall, the solid angle covered is increased considerably to about 1/3 of 4π. Also the number of events accumulated in the measured energy range was higher by an order of magnitude. Neutral particles were identified by time-of-flight and pulse-shape analyses. Details are given elsewhere [1–3].

In the photon energy range of this measurement the energies of deuterons and nucleons emitted from the reaction were too low for a significant detection (instrumental thresholds $E_d = 55$ MeV, $E_p = 40$ MeV, $E_n \approx 30$ MeV) in coincidence with the gammas from π^0 decay. For neutrons, in addition, the detection efficiency is not known well enough. Due to this and also due to an appreciable loss of acceptance by the constraint of particle coincidences, the coherent ($\gamma d \rightarrow \pi^0 d$) and incoherent ($\gamma d \rightarrow \pi^0 np$) channels could not be separated directly by an additional detection of d, p or n. However, they could be identified by fitting the missing energy spectra (fig. 3) with Monte Carlo (MC)-generated line shapes, provided the statistical accuracy in each 20° wide angular bin was sufficient. This required a tagged photon bin width $\Delta E_\gamma = \pm 10$ MeV near threshold [3] but $\Delta E_\gamma = \pm 1$ MeV was sufficient for high photon energies.

The obtained experimental results are shown in figs. 4-9 together with their statistical uncertainties. The systematic uncertainties in the absolute normalization of the cross-section are less than 7% [3]. Since for the separation of coherent and incoherent π^0 production channels MC-generated line shapes had to be used, this separation is not completely model independent. From using various reaction models (see discussion in sect. 4) we find this model dependence in the separation to be very small, in the order of 5% [3].

3 Experimental results

Figures 4-9 show the experimental results for angular and energy dependence of the coherent, incoherent and inclusive cross-sections for π^0 photoproduction from the deuteron in the energy range $E_\gamma \leq 306$ MeV. Angular distributions are shown only for a selection of incident energies. The full data are given in ref. [3].

For the coherent production there are just the previous TAPS data [1] plus a few fragmentary data from earlier experiments [4,5] to compare with. They were obtained primarily at large π^0 angles and are shown in fig. 4

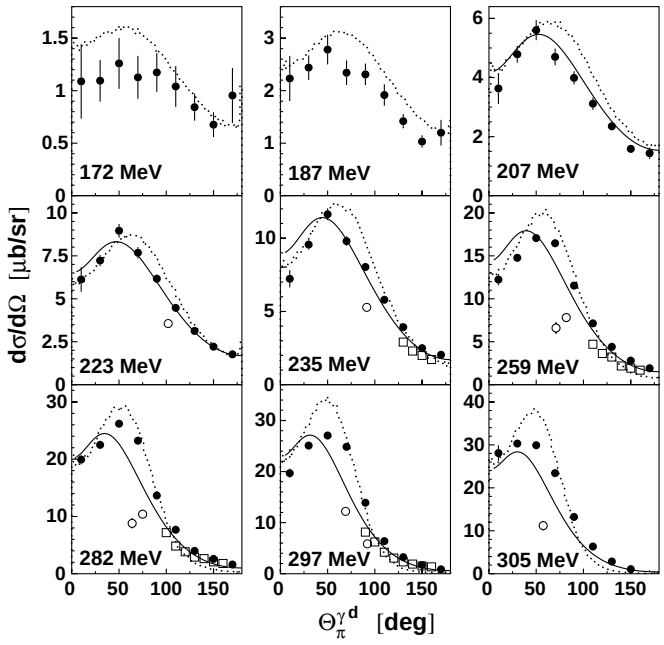

Fig. 4. Differential cross-sections for the coherent process $\gamma d \to \pi^0 d$ shown for a selection of incident photon energies. Data represented by open circles are from Bouquet *et al.* [5], open squares from Holtey *et al.* [4] and full circles from this work. The solid lines show results of a calculation by Kamalov *et al.* [12], the dotted lines results from our MC simulation based on the coalescence model with $q_0 = 300$ MeV/c.

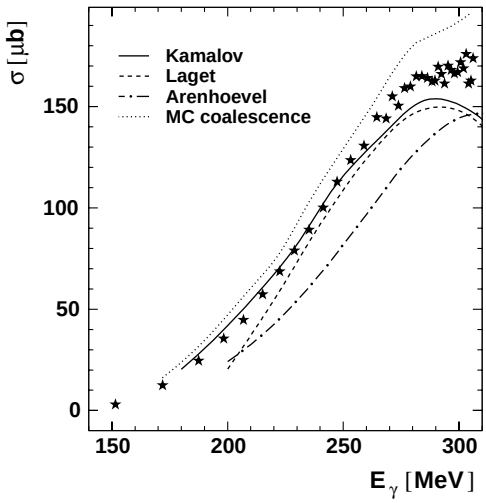

Fig. 5. Angle-integrated cross-sections for the coherent process $\gamma d \to \pi^0 d$ in the measured energy range $E_\gamma \leq 306$ MeV. Stars show the measurements of this work. They are compared to theoretical calculations of Kamalov *et al.* [12] (solid curve), Laget [11] (dashed), Arenhövel *et al.* [10] (dash-dotted) as well as to MC simulations based on a coalescence model (see text) with $q_0 = 300$ MeV/c (dotted).

by open symbols. Whereas the coherent production is strongly forward peaked in its angular dependence, the incoherent production appears to be peaked at backward angles (fig. 6). For the latter there are only the previous TAPS data [1] to compare with and within statistics they are in good agreement.

The inclusive cross-section, *i.e.* the sum of coherent and incoherent cross-sections, exhibits an angular dependence (fig. 8), which essentially is symmetric about 90° except at the lowest energies. This is consistent with the dominant contribution originating from a single partial wave, the resonant M_{1+} amplitude, and resembles very much the situation for π^0 production on the nucleon [6].

For $E_\gamma < 160$ MeV, *i.e.* near the pion threshold, there exist data of high statistical accuracy for the inclusive cross-section from measurements [7] at SAL. They are compared in fig. 9 to the results of this experiment. Within the statistics of the individual energy bins the data agree well with each other. However, over the full overlap range there is a clear trend that the SAL results lie high by about 10% compared to our results, *i.e.* we find here a similar discrepancy between the data sets of both installations as observed for $\gamma p \to \pi^0 p$ [8]. For $E_\gamma \geq 207$ MeV there exist previous TAPS measurements [1] with poorer statistics in the overlap region. The cross-sections obtained there are in good agreement with the present results both for the angular dependence and the integral values (fig. 9).

Finally, we note that the statistics in the present measurement of the total π^0 production cross-section are good enough to allow a sensitive search for narrow dibaryons. A detailed investigation of the data on this matter has been published previously [9].

4 Discussion of the data

i) Coherent production channel $d(\gamma, \pi^0)d$.
The data for coherent production are compared in figs. 4 and 5 to theoretical calculations of Arenhövel *et al.* [10], Laget [11] and Kamalov *et al.* [12]. The experimental energy dependence is reproduced best by the latter calculations, which also give a near quantitative description of the experimental angular distributions, in particular for $E_\gamma \leq 260$ MeV.

Also shown in figs. 4 and 5 are Monte Carlo (MC) simulations, which we carried out in the coalescence model [13–15]. In its simplest form it assumes that following a quasi-free process on one of the target nucleons the two nucleons recombine into the deuteron, if $q < q_0$ (with $\mathbf{q} = \mathbf{q}_1 - \mathbf{q}_2$ being the relative momentum of the outgoing nucleons), whereas for $q \geq q_0$ the deuteron breaks up and populates the incoherent exit channel. Utilizing the Hulthen wave function for the deuteron φ_d and SAID [16] amplitude $f_{\gamma\pi N}$ for the elementary process $\gamma N \to \pi^0 N$ these MC simulations provide a surprisingly good description of the experimentally observed energy and angular dependences both for the coherent and the incoherent channel. This calculation has only a single parameter, q_0, which has been adjusted to $q_0 \approx 300$ MeV/c for a reasonable description of the data. We note that this value is close to the one obtained for high-energy proton-nucleus collisions [13]. For the angle-integrated cross-sections displayed in figs. 5 and 7

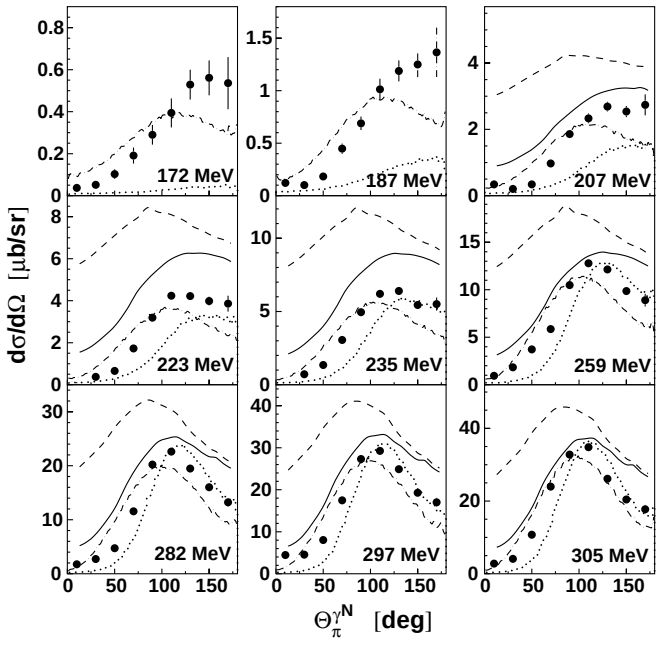

Fig. 6. Differential cross-section for the π^0 angular dependence of the incoherent process $\gamma d \rightarrow \pi^0 pn$ given in the photon-nucleon c.m. frame for a selection of incident photon energies. Full circles represent the measurements of this work. Solid and dashed curves show results of theoretical calculations by Laget [11] with and without FSI. The dotted lines represent MC simulations based on the coalescence model with $q_0 = 300$ MeV and the dash-dotted lines MC simulations based on the more realistic ansatz of Kolybasov and Ksenzov [17] for the NN-FSI.

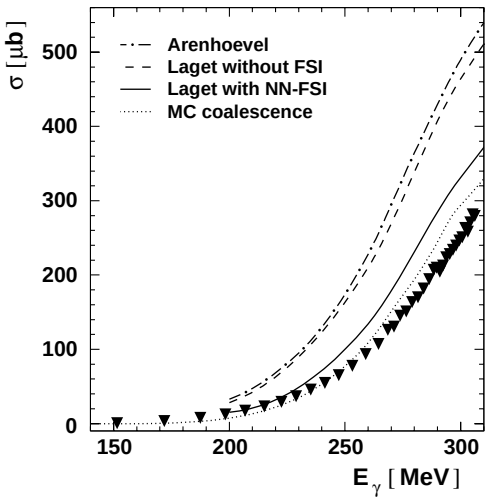

Fig. 7. Angle-integrated cross-sections for the incoherent process $\gamma d \rightarrow \pi^0 pn$ in the measured energy range $E_\gamma \leq 306$ MeV. Full triangles show the measurements of this work. They are compared to theoretical calculations of Laget [11] with (solid curve) and without (dashed) FSI, Arenhövel [10] (dash-dotted) and to MC simulations based on the coalescence model with $q_0 = 300$ MeV/c (dotted).

the coalescence model calculations are shown without any renormalization. For the angular distributions displayed in figs. 4 and 6 the coalescence model calculations have been slightly renormalized energy-by-energy to the angle-integrated data for the total π^0 production cross-section (fig. 9), which is just the sum of coherent and incoherent production cross-sections. We also note that simple PWIA calculations [3], where the SAID amplitudes for $\gamma N \rightarrow \pi^0 N$ are multiplied with the experimental deuteron form factor, give angular distributions for the coherent channel which, too, are very close to those of the coalescence model and those also of Kamalov *et al.* From this we conclude that the bulk properties of the coherent channel are well understood.

ii) Incoherent production channel $d(\gamma, \pi^0)pn$.
The situation is somewhat more complicated for the incoherent or break-up channel. In the absence of any final state interaction the channel would be associated with the quasi-free π^0 production on the nucleons. However, quasi-free calculations fail badly. For the angular distributions such calculations predict a shape symmetric about 90° (dashed curves in fig. 6 and dashed and full curves in fig. 8), which is not observed experimentally. Also for the energy excitation function they predict much too large a cross-section (dashed and dash-dotted curves in fig. 7). As already pointed out by Laget [11], the break-up channel is strongly influenced by NN-FSI, which greatly reduce the break-up cross-section by about 30% and cause its angular distributions to be backward peaked (solid curves in figs. 6 and 7). These findings are also corroborated by the results of the coalescence model discussed above. In order to improve this sharp cut-off model towards a more realistic smooth transition, we have carried out MC simulations, where instead of the sharp cut-off parameter q_0 the parameter-free NN-FSI of Kolybasov and Ksenzov [17] has been used.

In ref. [17] the connection between coherent and break-up processes on the deuteron has been evaluated. By use of the completeness relation, it has been shown therein that the sum of the coherent cross-section and the cross-section for the quasi-free process including FSI gives the pure quasi-free cross-section, (*i.e.* without FSI). This means that the effect of the FSI in the break-up process just counterbalances the coherent process. Following ref. [17], we may write the expression for the rescattering graph shown in fig. 1c as

$$M_{\mathrm{R}} = \frac{f_{\gamma\pi p} + f_{\gamma\pi n}}{\pi^2} \int \mathrm{d}\mathbf{q}' \; \frac{f_{NN}(\mathbf{q}, \mathbf{q}') \; \varphi_d(\mathbf{q}' - \mathbf{Q})}{q'^2 - q^2 - i\varepsilon} \; , \quad (1)$$

where $f_{\gamma\pi N}$ stands for the amplitude $\gamma N \rightarrow \pi N$ and f_{NN} is the s-wave elastic NN amplitude, which takes into account that the two nucleons before rescattering are off-mass-shell; $\mathbf{q}'$ and $\mathbf{q}$ are relative nucleons momenta before and after rescattering, respectively; $\mathbf{Q}$ is momentum transfer; $q = |\mathbf{q}|$, $q' = |\mathbf{q}'|$, $Q = |\mathbf{Q}|$.

The amplitude M_{R} is normalized in the same way as in ref. [17], and f_{NN} is normalized so that for two nucleons on mass shell $\mathrm{d}\sigma_{NN}/\mathrm{d}\Omega = |f_{NN}^{(\mathrm{on})}|^2$. The pure quasi-free

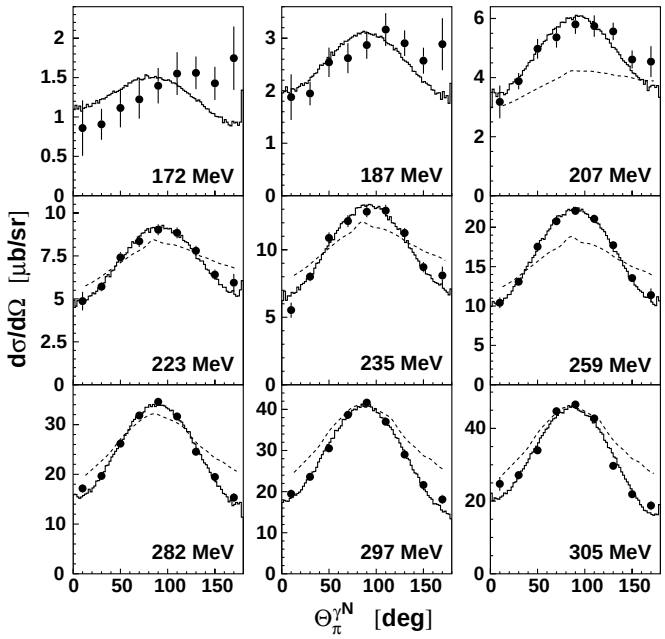

Fig. 8. Differential cross-sections for the inclusive π^0 photoproduction process $\gamma d \to \pi^0 X$ for a selection of incident photon energies. Solid and dashed lines show the pure quasi-free cross-sections from our MC simulations and from calculations by Laget [11], respectively. The latter are identical to those shown as dashed curves in fig. 6. Our MC simulations have been renormalized energy-by-energy to the angle-integrated data.

amplitude $\gamma d \to \pi^0 np$ is given by

$$M_{\rm QF} = f_{\gamma\pi p}\varphi_d\left(\mathbf{q}-\mathbf{Q}\right) + f_{\gamma\pi n}\varphi_d\left(\mathbf{q}+\mathbf{Q}\right) \ . \qquad (2)$$

The summary contribution of the diagrams shown in fig. 1b and fig. 1c can then be written as

$$M_{\rm FSI} = M_{\rm QF} + M_{\rm R} = M_{\rm QF}[1 + R^{-1} f_{NN}^{(\rm on)}] \ , \qquad (3)$$

where

$$R^{-1}(\mathbf{q},\mathbf{Q}) = \frac{f_{\gamma\pi p} + f_{\gamma\pi n}}{M_{\rm QF}} * \\ * \int \frac{{\rm d}\mathbf{q}'}{\pi^2} \ \frac{4q^2+\beta^2}{4q'^2+\beta^2} \ \frac{\varphi_d(\mathbf{q}'-\mathbf{Q})}{q'^2-q^2-i\varepsilon} \ .$$

Integration over $\mathbf{q}'$ with the Hulthen wave function gives

$$R^{-1}(\mathbf{q},\mathbf{Q}) = \frac{4\alpha}{q} \ \frac{f_{\gamma\pi p} + f_{\gamma\pi n}}{M_{\rm QF}} \ [I(\kappa) - I(\beta)] \ , \qquad (4)$$

where $\kappa^2 = mE_d$ with E_d being the deuteron binding energy and m the nucleon mass; $\beta = 5.2\kappa$; α is the normalization factor of the Hulthen wave function:

$$\alpha = 4\pi \left[\frac{\kappa\beta(\kappa+\beta)}{2\pi(\beta-\kappa)^2}\right]^{\frac{1}{2}} \ , \qquad (5)$$

and function $I(x)$ is equal to

$$I(x) = \frac{i}{2}\left[\ln\frac{q+Q+2ix}{q-Q+2ix} - \ln\frac{i\beta+Q+2ix}{i\beta-Q+2ix}\right] \ . \qquad (6)$$

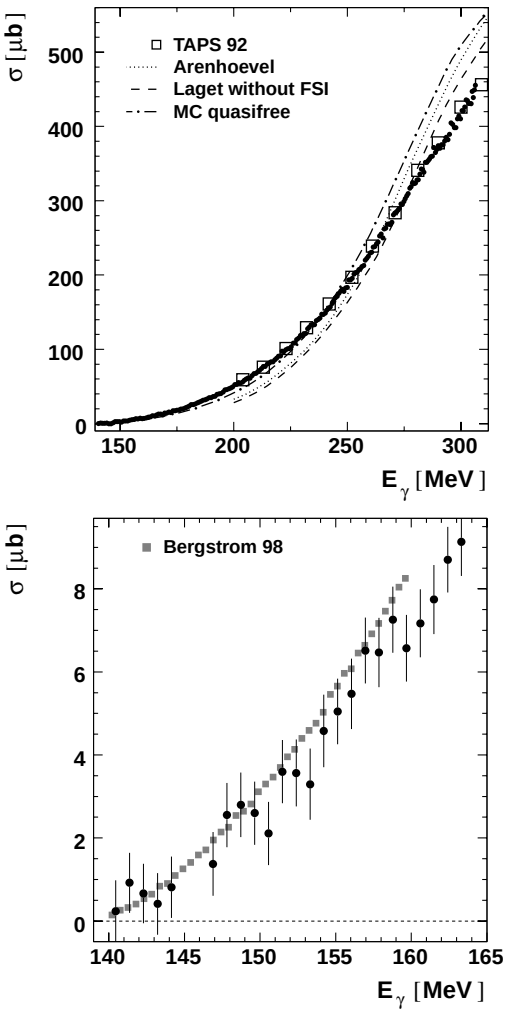

Fig. 9. Angle-integrated cross-sections for the inclusive π^0 photoproduction process $\gamma d \to \pi^0 X$ in the measured energy range $E_\gamma \leq 306$ MeV. Solid circles show the measurements of this work. They are compared to data from Bergstrom *et al.* [7] (solid squares, bottom) and to previous TAPS results [1] (open squares, top). The data are also compared to theoretical calculations of Arenhövel [10] (dotted), Laget [11] without FSI, *i.e.* purely quasi-free (dashed, identical to the dashed curve in fig. 7) and to MC simulations of the pure quasi-free process using SAID amplitudes with renormalization (dot-dashed).

Our MC simulations including this FSI are shown in fig. 6 by the dash-dotted curves. In shape these results are quite similar to the ones of Laget including FSI. In absolute magnitude they are below the latter (and in better agreement with the data), since the MC simulations have been renormalized energy-by-energy to reproduce the angle-integrated total cross-sections (see the discussion below).

iii) Inclusive π^0 production $d(\gamma,\pi^0)X$.
The angular distributions of the inclusive cross-section are compared in fig. 8 to quasi-free calculations by Laget [11] and our MC simulations assuming a quasi-free process utilizing just the Hulthen wave function and SAID

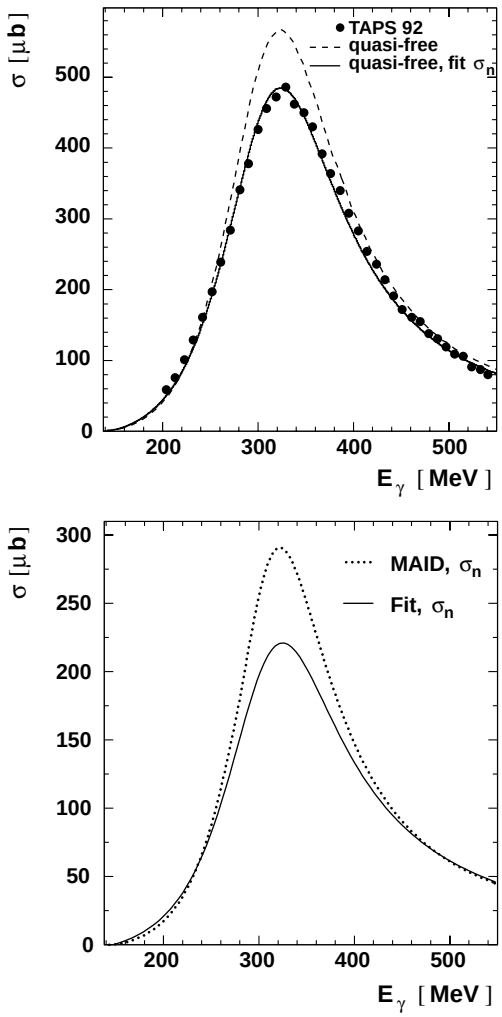

Fig. 10. Top: angle-integrated cross-sections for the inclusive π^0 photoproduction process $\gamma d \to \pi^0 X$ in the energy range $E_\gamma < 600$ MeV. The data (solid circles) are from the previous TAPS experiment [1]. They are compared to the MC simulations of the pure quasi-free process. The dashed curve shows the result when the MAID [18] cross-sections for both $\gamma p \to \pi^0 p$ and $\gamma n \to \pi^0 n$ (bottom, dotted) are used. The solid curve is the result when the $\gamma n \to \pi^0 n$ cross-sections in the MC simulations are reduced as shown in the bottom figure by the solid curve. Bottom: comparison between the $\gamma n \to \pi^0 n$ cross-section from MAID (dotted) and that needed for a reasonable description of the data (solid line).

amplitudes. After renormalizing these simulations energy-by-energy to the angle-integrated cross-sections, *i.e.* the total π^0 production cross-sections, the agreement to the data in fig. 8 is very good, except for the lowest energy bin. This excellent agreement in the angular dependence of the quasi-free process with the data is in full accord with the statement of ref. [17] discussed above, that coherent and incoherent cross-sections add up to the quasi-free cross-section, which is therefore seen in the inclusive cross-section. The same conclusion has been reached by Laget [11].

In turn, if this conclusion is correct, then the energy dependence of the total π^0 production cross-section should also be represented quantitatively by the quasi-free process. However, this is not the case for $E_\gamma \gtrsim 250$ MeV, as can be seen in fig. 9 by comparing the dash-dotted curve with the data. In fig. 10 the TAPS data [1] obtained recently over the full Δ-resonance region are compared to the MC simulations of the quasi-free process. As can be seen, this process overshoots the data for $E_\gamma \gtrsim 250$ MeV by up to 15% at the maximum of the Δ-resonance excitation. Since the $\gamma p \to \pi^0 p$ cross-sections are well established, the only possible uncertainties in the calculation of the quasi-free process are the $\gamma n \to \pi^0 n$ cross-sections. The latter have been taken from the SAID and MAID [18] phase shift analyses, respectively. Whereas in the SAID analysis proton and neutron cross-sections are nearly identical in the region of the Δ-resonance, the neutron cross-sections are smaller by about 3% near the top of the Δ excitation in the MAID analysis.

In order to reproduce the data by the quasi-free calculation, the MAID neutron cross-sections had to be reduced by up to 25% between $E_\gamma \gtrsim 250$ and 450 MeV (fig. 10, bottom). This is surprising, since no large isospin asymmetry is known for the excitation of the Δ-resonance. Hence, this reduction would need to be associated with background terms in the π^0 photoproduction on the nucleon. Isoscalar contributions, which enter the $\gamma n \to \pi^0 n$ and $\gamma p \to \pi^0 p$ amplitudes with different signs, could possibly be the origin for the observed differences. As discussed above, the decrease of the break-up cross-section due to NN-FSI ought to be compensated just by the coherent channel cross-section, so that their sum, the total π^0 production cross-section, is represented by the pure quasi-free process. This compensation, however, is exact only:

- if the full NN phase space is available, so that the completeness relation is satisfied. This condition is well fulfilled at high energies. It is still nearly fulfilled at our energies, since the range of momenta of the outgoing nucleons is already large compared to the Fermi momentum of the nucleons inside the deuteron.
- in the isoscalar np channel, not in the isovector channel. However, if the π^0 is produced via the Δ mechanism —as is the case preferentially in the Δ region— then isospin selection allows only isoscalar np pairs. This again points to the background terms in the π^0 production as a possible origin for the observed discrepancy in the Δ region. Though only a full coupled channel treatment can give a quantitative estimate of these effects, they are not expected to affect the total π^0 production cross-section by more than a few percent and hence are unlikely to fully explain the observed discrepancy.

An alternative explanation could principally be that the total π^0 production process gets reduced by strong coupling to the deuteron photodisintegration channel. However, it is not obvious why this should happen just for $E_\gamma > 250$ MeV and why this should have no influence on the angular dependence. Above pion threshold the photodisintegration process cross-section is largest

(70 μb) near $E_\gamma \approx 280$ MeV and decreases quite rapidly towards higher energies. At $E_\gamma \approx 330$ MeV, where we find the largest discrepancies, the photodisintegration cross-section has already dropped by nearly a factor of two. Also the calculations of Laget, which include this channel, do not show such a strong coupling effect. Finally, the final-state πN rescattering with its possibility of pionic charge exchange would have the potential of lowering the total cross-section. Again, it is not obvious why this should only happen in the Δ-resonance region. Furthermore, even there the πN scattering amplitude is an order of magnitude smaller than the s-wave NN scattering amplitude. Hence, it is not surprising that the πN rescattering contributions are much smaller than the NN ones as borne out again quantitatively by Laget's calculations.

As seen from fig. 10, for $450\,\text{MeV} \lesssim E_\gamma \lesssim 550\,\text{MeV}$ the quasi-free calculations based on SAID/MAID amplitudes come again close to the data. We note, however, that for $550\,\text{MeV} \leq E_\gamma \leq 800$ MeV these calculations again exceed the TAPS data by up to 40% [19].

5 Summary

The new data on coherent, incoherent and inclusive π^0 photoproduction from the deuteron fill the gap between the pion threshold and the Δ-resonance region, where data are available from previous measurements. For $E_\gamma < 160$ MeV our data are in reasonable agreement with the high-statistics measurements [7] of the inclusive cross-section at SAL, though the latter lie systematically somewhat higher. At the high-energy end the new data are in good agreement with the previous poorer statistics TAPS data [1].

The coherent production is strongly peaked towards forward angles. This may be easily understood because of the small relative momenta between the nucleons in deuterium. For larger momenta the deuteron breaks up and feeds the incoherent channel, where therefore the angular distributions are backward peaked. These features are borne out by the MC simulations using the simple coalescence model or more realistically by using the FSI ansatz of ref. [17] as well as by the theoretical calculations of Laget [11].

The angular dependence of the inclusive $d(\gamma,\pi^0)X$ reaction is quantitatively reproduced by the pure quasi-free process as predicted by Laget [11] and Kolybasov [17]. However, for $E_\gamma > 250$ MeV, the observed absolute cross-sections are lower than the predictions for the quasi-free process. If this discrepancy is associated with the $\gamma n \to \pi^0 n$ process, then its cross-section would need to be reduced by up to 25%.

Supported by the BMBF under contract 06 TU 886, the DFG (Mu 705/3, Graduiertenkolleg and SFB 201) and DAAD (Euler program).

References

1. B. Krusche *et al.*, Eur. Phys. J. A **6**, 309 (1999).
2. A.R. Gabler *et al.*, Nucl. Instrum. Methods A **346**, 168 (1994).
3. U. Siodlaczek, Doctoral Thesis, University of Tübingen, 2000; `http://www.w210.ub.uni-tuebingen.de/dbt/volltexte/2001/213`.
4. G. Holtey *et al.* Z. Phys. **259**, 51 (1973).
5. B. Bouquet *et al.*, Nucl. Phys. B **79**, 45 (1974).
6. M. Fuchs *et al.*, Phys. Lett. B **368**, 20 (1996).
7. J.C. Bergstrom *et al.*, Phys. Rev. C **57**, 3203 (1998).
8. A.M. Bernstein *et al.*, Phys. Rev. C **55**, 1509 (1997).
9. U. Siodlaczek *et al.*, Eur. Phys. J. A, accepted for publication.
10. H. Arenhövel, P. Wilhelm, Nucl. Phys. A **593**, 435 (1995).
11. J.P. Laget, Phys. Rep. **69**, 1 (1981).
12. S.S. Kamalov, L. Tiator, C. Bennhold, Phys. Rev. C **55**, 98 (1997).
13. A. Schwarzschild, Č. Zupančič, Phys. Rev. **129**, 854 (1963).
14. S.T. Butler, C.A. Pearson, Phys. Rev. Lett. **7**, 69 (1961); Phys. Lett. **1**, 77 (1962); Phys. Rev. **129**, 836 (1963).
15. H. Machner, Phys. Rep. **127**, 309 (1985).
16. Program package SAID, R.A. Arndt *et al.*, `http://www.vtinte.phys.vt.edu`; see also R.A. Arndt, Phys. Rev. D **28**, 97 (1983).
17. V.M. Kolybasov, V.G. Ksenzov, Sov. J. Nucl. Phys. **22**, 372 (1976).
18. Program package MAID, L. Tiator, `http://www.kph.uni-mainz.de/MAID`; see also D. Drechsel *et al.*, Nucl. Phys. A **645**, 145 (1999).
19. B. Krusche, Czech. J. Phys. **50/54**, 24 (2000).